Construction and Building Materials 247 (2020) 118543 (https://doi.org/10.1016/j.conbuildmat.2020.118543)
Article history:
Received 26 February 2019
Received in revised form 13 January 2020
Accepted 22 February 2020

Low cost and sustainable repair material made from alkali-activated high-calcium fly ash with calcium carbide residue

Tanakorn Phoo-ngernkham[a,*], Chattarika Phiangphimai[a], Darakorn Intarabut[a], Sakonwan Hanjitsuwan[b], Nattapong Damrongwiriyanupap[c], Long-yuan Li[d] and Prinya Chindaprasirt[e,f**]

[a] *Sustainable Construction Material and Technology Research Unit, Department of Civil Engineering, Faculty of Engineering and Architecture, Rajamangala University of Technology Isan, Nakhon Ratchasima 30000, Thailand*

[b] *Program of Civil Technology, Faculty of Industrial Technology, Lampang Rajabhat University, Lampang 52100, Thailand*

[c] *Civil Engineering Program, School of Engineering, University of Phayao, Phayao 56000, Thailand*

[d] *School of Engineering, Faculty of Science and Engineering, Plymouth University, PL4 8AA, United of Kingdom*

[e] *Sustainable Infrastructure Research and Development Center, Dept. of Civil Engineering, Faculty of Engineering, Khon Kaen University, Khon Kaen 40002, Thailand*

[f] *Academy of Science, The Royal Society of Thailand, Dusit, Bangkok 10300, Thailand*

Abstract

In this work, a study on a low cost and sustainable repair material made from alkali-activated high-calcium fly ash (FA) incorporated with calcium carbide residue (CCR) is reported. The FA was partially replaced with CCR (additional calcium source) at the dosages of 0%, 10%, 20%, and 30% by weight of binder. The alkaline activators were sodium silicate

(SS) and sodium hydroxide (SH) solutions with SS-to-SH ratios of 1.0, 1.5, 2.0 and 2.5 by weight. The alkali activator liquid/solid binder (FA+CCR) ratio of 0.60 and curing at 25 ^{o}C (ambient temperature) were used for all mixes. Experimental results showed that the setting time of mortar decreased with increases of CCR replacement level and SS-to-SH ratio, whereas the strength development increased. XRD and SEM results demonstrated that an optimum level of CCR replacement and SS-to-SH ratio resulted in the additional formation of C-S-H (calcium silicate hydrate) and/or C-A-S-H (calcium aluminosilicate hydrate) that coexisted with N-A-S-H (sodium aluminosilicate hydrate). The bond strength of the alkali-activated mortar with concrete substrate was also improved. The setting time and strengths complied with the requirement of the ASTM standards for repair materials and thus indicated its suitable as an alternative repair material in terms of environmentally friendly and low cost.

Keywords: Low cost; Sustainable repair material; Alkali-activated binder; High-calcium fly ash; Calcium carbide residue.

---

[*] *Corresponding author. Tel: +66 4423 3000 ext.3210; E-mail address: tanakorn.ph@rmuti.ac.th*

[**] *Corresponding author. Tel: ++66 4320 2355; E-mail address: prinya@kku.ac.th*

1. Introduction

Nowadays, great effort has been made to develop alternative cement for replacing ordinary Portland cement (OPC). The production of OPC releases a large quantity of CO_2 [1]; approximately 1 ton of CO_2 for every ton of OPC [2]. Therefore, alternative low-carbon products have to be explored to reduce greenhouse gas, for instance, the use of supplementary cementitious materials [3], calcined clay-limestone cements [4] and alkali-activated binders [5-9]. Recently, alkali-activated binders are receiving more attention as an alternative cementitious material to OPC because of its advantages over OPC in terms of low CO_2

emission [10], excellent resistance to acid and sulfate [11, 12], good bond with reinforcing steel [13, 14], high fire resistance [15] and excellent bond with old concrete [16-18].

Alkali-activated (AA) binder is obtained from aluminosilicate materials activated with concentrated alkali solutions such as sodium hydroxide (SH) solution and sodium silicate (SS) solution [19]. As per the publication of Pacheco-Torgal et al. [7], it was suggested that AA binders could be classified into two categories. One is the blast furnace slag activated with a mild alkaline solution. The other is the metakaolin or low calcium FA activated with medium or high alkaline solutions. The former has a combination of C-S-H (calcium silicate hydrate) and/or C-A-S-H (calcium aluminosilicate hydrate) and N-A-S-H (sodium aluminosilicate hydrate) gels as the main products, whereas the latter has only N-A-S-H gel [7, 20]. The reaction product of N-A-S-H gel gives lower strength than a combination of N-A-S-H and C-S-H gels as reported in many publications [21-24]. In Thailand, the high-calcium FA from Mae Moh power plant in northern Thailand is the most widely used source material for AA binders. The high calcium content from FA is essential to improve the strength development of AA binder when cured at room temperature [18, 24-28]. The reaction of calcium oxide and mild alkali solution generates heat [7] and is therefore beneficial to an enhancement of mechanical properties of AA binder.

The AA high-calcium FA has been used as an alternative repair material [16-18, 29] because of its fast setting and excellent mechanical properties. However, its strength is still lower than that of alkali-activated slag incorporated with low calcium FA [24]. Many researchers have used the reactive CaO as additives for developing its strength when cured at ambient temperature. For instance, FA was replaced or blended with OPC [16, 28, 30], calcium hydroxide [17] and gypsum [31, 32]. The other interesting calcium rich waste material is the calcium carbide residue (CCR) from acetylene production process. It is attractive for use as calcium promoter to enhance the strength development because CCR

involves a high calcium hydroxide ($Ca(OH)_2$) content [33]. As reported in literature, $Ca(OH)_2$ from CCR reacts with SiO_2 and Al_2O_3 from high-calcium FA to form additional reaction product [34] and hence leads to better overall strength development. Therefore, the use of CCR with high alkalinity is attractive in terms of both the economical and environmental perspectives because it helps to reduce substantially environmental problem [35]. Many researchers have used CCR with high-calcium FA for making AA binders. For example, Phummiphan et al. [36] studied the marginal lateritic soil stabilized with CCR and high-calcium FA for developing sustainable pavement. Phetchuay et al. [37] used high-calcium FA geopolymer with CCR as a sustainable material to improve the strength of soft marine clay. However, there is not much work on CCR used as the repair material for repairing damaged concrete, in which case not only the compressive strength but also the setting time and bond strength are the crucial design parameters.

Therefore, the aim of this paper is to study the setting time and strength of AA high-calcium FA mortar incorporated with CCR. The AA high-calcium FA-CCR paste was analyzed using XRD and SEM. The compressive strength and shear bond strength were tested. The effect of SS-to-SH ratio on the strength development of AA high-calcium FA mortar with CCR was also investigated. The obtained knowledge would be instrumental for the future application of AA high-calcium FA paste and mortar incorporated with CCR as alternative repair materials.

2. Experimental details

2.1 Materials

In this study, the precursors were the lignite coal FA obtained from Thailand Mae Moh power plant and the CCR obtained from an acetylene gas process in Sai 5 Gas Product Co., Ltd. The CCR was dried in the oven at 100^oC for 24 hours because it had a high moisture

content approximately 52% [34]. Then, it was ground using a Los Angeles abrasion machine to obtain fine particles by passing a sieve No. 100 (150 μm). After grinding, the CCR was covered using plastic sheet to prevent moisture exchange. The CCR had the specific gravity of 2.25, median particle size of 21.2 μm, and Blain fineness of 4550 cm^2/g. The FA had the specific gravity of 2.64, median particle size of 15.5 μm, and Blain fineness of 4300 cm^2/g. Figure 1 shows the particle size distributions of the CCR and FA used. A 10M SH solution and a SS solution with 11.67% Na_2O, 28.66% SiO_2 and 59.67% H_2O were used as liquid activators with a fixed liquid alkaline to binder ratio of 0.60. In the present study, different SS/SH ratios were also used in the mixtures to examine the effect of SS/SH ratio on the setting time, mechanical strengths and microstructure of AA high-calcium FA with CCR. Table 1 gives the chemical compositions of FA and CCR. The FA consisted mainly of SiO_2, Al_2O_3, Fe_2O_3, CaO with some other minor elements. The sum of SiO_2, Al_2O_3 and Fe_2O_3 was 60.96%, with 25.79% CaO complied with Class C fly ash as per ASTM C618-15 [38]. While, the CCR mainly consisted of ~~high calcium content ($Ca(OH)_2$ and/or~~ CaO~~)~~ (89.2%) with some components of SiO_2 (6.16%), Al_2O_3 (3.54%) and LOI (2.79%). Local river sand of sizes ranging from 0.07 mm to 3 mm with 2.63 specific gravity and 1.80 fineness modulus was used for producing mortar samples.

For the mixing of the mortar, FA, CCR and fine aggregate were mixed together for 60s. After that, SS and SH solutions were added, and then mixed again for 30s. The mix proportions of AA high-calcium FA with CCR mortar is shown in Table 2. Note that due to different densities of individual components the overall densities of the mixed pastes and/or mortars are also different. The mixing of pastes for the SEM and XRD analyses was the same as that of mortar but without adding the river sand.

2.2 Testing and analysis

After mixing, the setting time of AA high-calcium FA with CCR was evaluated using the method of penetration resistance as per ASTM C191 [39]. After that, a fresh mortar was placed into 50x50x50 mm cube molds for the compressive strength test of mortar as per ASTM C109 [40]. While, the shear bond strength between the mortar and Portland cement concrete substrate (PCC) was tested using slant shear. The test was adapted from ASTM C882 [41] as reported in previous studies [17, 18]. The details of PCC were given in the previous studies [18, 24, 42]. The PCCs were cut at an angle of 30° to the cross-section at the middle section for acting as a concrete substrate used for the shear bond strength test. The casting of samples was based on the previous studies [16-18, 24, 25]. The mortar was cast into a 50x50x125 mm prism mold containing the cut PCC sample. After that, the prisms were immediately covered using vinyl sheet and kept in a 25 ºC controlled room.

For the preparation of XRD samples, the 28-day alkali-activated paste cube was broken and ground to fine particles. The XRD was performed at 5 to 60 °2theta with an increment of 0.02 degree/step and a speed of 0.5 sec/step. The quantitative XRD analysis was performed by using Bruker's TOPAS software to determine amorphous phases. For the preparation of SEM samples, the 28-day alkali-activated paste cubes were broken and the middle portions of the cubes were used. The micrographs were recorded at 15 kV and 1,000x magnification.

3. Results and Discussion

3.1 Setting time

Figure 2 summarizes the results of the setting time of AA high-calcium FA mortar incorporated with CCR. It is evident that the CCR replacement level and SS-to-SH ratio mainly controlled the setting time of mortar. As is observed from the figure, the setting time tended to decrease with the increases of both CCR replacement and SS-to-SH ratio. For example, the final setting times of 100FA-SS/SH=1.0, 100FA-SS/SH=1.5, 100FA-

SS/SH=2.0, 100FA-SS/SH=2.5; 80FA20CCR-SS/SH=1.0, 80FA20CCR-SS/SH=1.5, 80FA20CCR-SS/SH=2.0 and 80FA20CCR-SS/SH=2.5 were 45, 41, 32, 28; 24, 21, 16 and 12 min, respectively. As the CCR contained a reasonably high calcium ($Ca(OH)_2$ and CaO) content of 89.24%, the rapid setting and hardening of mortar was obtained. Lee and Van Deventer [43] reported that the solidification rate was increased as a result of the extra nucleation sites for precipitation of dissolved species. This agreed with Pangdaeng et al. [30] that ~~the use of PC (contained a high CaO content at 65.3%) to replace FA for producing geopolymer mortar accelerated the setting of the mixture. Also, Pangdaeng et al. [30] suggested that~~ the heat generated by CaO assisted the geopolymerization process. According to Figure 2, the high SS-to-SH ratio shortened the setting time of mortar when compared to the low SS-to-SH ratio. This was because the reactive SiO_2 from SS solution reacted with ~~$Ca(OH)_2$~~ ~~and~~ CaO from high calcium FA and CCR. The fast setting of AA mortar is advantageous for repair material. As per ASTM C881/C881M-14 [44], the required initial setting time for repair binder must be less than 30 min. The results shown in Figure 2 indicate that all of the AA high-calcium FA mortars incorporated with CCR met the setting time requirement of ASTM standard.

3.2 Strength

3.2.1 Compressive strength

The results of compressive strength of AA high calcium FA mortars incorporated with CCR are shown in Figure 3. The compressive strengths of AA mortars increased with increasing CCR replacement level (except for the 30%CCR replacement). For example, the 28-day strengths of 100FA-SS/SH=2.0, 90FA10CCR-SS/SH=2.0, 80FA20CCR-SS/SH=2.0 and 70FA30CCR-SS/SH=2.0 were 51.8, 62.4, 64.6 and 54.8 MPa, respectively. Hanjitsuwan et al. [33] reported that the free $Ca(OH)_2$ and CaO from CCR reacted with silica and alumina from

FA and formed additional C-S-H and C-A-S-H. These results are consistent with the findings of Phoo-ngernkham et al. [26] and Pangdaeng el at. [30]. The slight strength loss of 30%CCR samples is probably due to the rapid chemical reaction of the matrix (confirmed with the results of setting time of mortar as shown in Figure 2), which causes the strength of the material not fully being developed. According to Figure 3, the SS-to-SH ratio also played a significant role on the strength development of mortar. For example, the 28-day strengths of 80FA20 CCR-SS/SH=1.0, 80FA20CCR-SS/SH=1.5, 80FA20CCR-SS/SH=2.0 and 80FA20CCR-SS/SH=2.5 were 53.1, 61.2, 64.6 and 57.3 MPa, respectively. This suggests that the strength of mortar increased with increasing SS-to-SH ratio up to a threshold level (SS/SH=2.0) and after then it started to decrease. This again is due to the fact that the setting of matrix being too fast would result in a formation of poor initial matrix structure and thus hinders the subsequent strength development [33]. Khater [45] also claimed that the excessive lime would have an adverse effect on the optimum gels binder structure. Nevertheless, according to Figure 3, the 7-day strengths of AA mortar met the strength requirement as per ASTM C928-13 [46]. In fact, all mixes of alkali-activated mortars met the 28-day strength requirement for repair material of ASTM C881/C881M-14 [44]. Therefore, the AA high-calcium FA mortar incorporated with CCR satisfies the strength requirement for the use as an alternative repair material.

3.2.2 Shear bond strength

The results of shear bond strength between AA mortar and PCC substrate are summarized in Figure 4. The 28-day shear bond strength between AA mortar and PCC substrate tended to increase with increasing CCR replacement and SS-to-SH ratio up to an optimum level. For example, the shear bond strengths for 100FA-SS/SH=1.0, 100FA-SS/SH=1.5, 100FA-SS/SH=2.0, 100FA-SS/SH=2.5; 80FA20CCR-SS/SH=1.0, 80FA20CCR-

SS/SH=1.5, 80FA20CCR-SS/SH=2.0 and 80FA20CCR-SS/SH=2.5, were 7.1, 8.7, 9.0, 7.3; 13.1, 14.6, 15.0 and 14.1 MPa, respectively. The noticeable increase in shear bond strength was observed when AA mortar contained the optimum amount of CCR. The reaction products at the contact zone were improved remarkably. Many researchers [16-18, 24, 25, 29, 47] have reported that additional C-S-H and/or C-A-S-H gel were formed and coexisted with N-A-S-H gel, which was the main reason for enhancing the bonding strength at contact zone. However, similar to the compressive strength, the bond strength of 30%CCR was also lower than that of 20%CCR, indicating that there is a turning point for the CCR addition. It was reported that large heat generated from $Ca(OH)_2$ and CaO from high-calcium FA and CCR with alkali medium had negative influence on the composite materials similar to that of the AA binder made from high-calcium FA incorporated with commercial calcium hydroxide [17]. Thus, care should be taken for the use of CCR, particularly when a higher SS-to-SH ratio is used in order to keep the balance between the setting time and strength development. Concerning the effect of SS-to-SH ratio, the shear bond strength increased with increasing SS-to-SH ratio up to 2.0 and beyond this it started to decrease, suggesting that the SS-to-SH ratio should not exceed 2.0, which is consistent with the compressive strength. The high shear bond strengths were observed in the mixes of 100FA-SS/SH=2.0, 90FA10CCR-SS/SH=2.0, 80FA20CCR-SS/SH=2.0 and 70FA30CCR-SS/SH=1.5 for all CCR replacement levels.

The shear bond strength of a few available commercial repair materials (CRM) was also tested. CRM-1 was general purpose non-shrink grout mortar, whereas CRM-2 was polymer modified repair mortar. It can be seen that the mixes of AA mortar showed lower bond strength than that of CRM-1 (22.0 MPa) but higher than that of CRM-2 (14.0MPa). Nonetheless, the shear bond strengths of AA mortars met the minimum bonding strength requirement (10 MPa) as per ASTM C881/C881M-14 [44]. Therefore, the AA high-calcium FA mortar incorporated with CCR has a good potential for the use as an alternative repair material.

3.3 XRD analysis

Figures 5-8 summarize the results of the XRD patterns of the AA high-calcium FA paste incorporated with CCR. The XRD patterns of the paste without CCR under different SS-to-SH ratios are illustrated in Figures 5a, 6a, 7a and 8a, respectively. It can be seen from the figures that there were amorphous phases shown by the hump around 20-38° 2theta and crystalline phases of quartz (SiO_2), magnetite (Fe_2O_3), mullite ($Al_6Si_2O_{13}$), calcite ($CaCO_3$) and C-S-H. It has been reported that the presence of amorphous phases in the XRD pattern corresponded to the combination of C-S-H and N-A-S-H gels within the matrix [49]. This reaction product controls the strength development of AA cement [7].

For the mixes with 10%CCR at the SS-to-SH ratio of 1.0, the pattern was similar to the pastes without CCR, as illustrated in Figure 5b. While for the 80FA20CCR-SS/SH=1.0 (Figure 5c) and 70FA30CCR-SS/SH=1.0 (Figure 5d), the peaks of aluminite ($Al_2(SO_4)(OH)_4.17H_2O$) and vishnevite ($Na_8Al_6Si_6O_{24}(SO_4)_2.H_2O$) were noticed ~~with a reduction in quartz (SiO_2)~~. Noticeable difference was also found in the mixes with CCR at SS-to-SH ratios of 1.5, 2.0 and 2.5 as shown in Figures 6b-6d, 7b-7d, 8b-8d. ~~A shift in the hump to a broad hump at 25-35 °2theta with~~ The crystalline phases of quartz (SiO_2), magnetite (Fe_2O_3), mullite ($Al_6Si_2O_{13}$), calcite ($CaCO_3$), C-S-H and $Ca(OH)_2$ were observed. The associated increase in peaks of portlandite, C-S-H, and broad hump is similar to the behaviors of AA high-calcium FA containing PC [17, 30]. Phoo-ngernkham et al. [24] reported that a large amount of amorphous phase with C-S-H gel was responsible for the increase in strength development of alkali-activated binders (see Figure 3). However, in the sample of 30%CCR replacement there was high amount of portlandite and calcite. When the water was not sufficient there the formed portlandite might not be fully hydrated, which could affect the compressive and bond strength development.

3.4 SEM analysis

The SEM images of AA paste cured for 28 days are shown in Figure 9. It can be seen that, the SEM images corresponded well to the strength behaviors (see Figure 3). The SEM image appeared dense with increasing CCR replacement and SS-to-SH ratio except for the mixes of 70FA30CCR or SS/SH=2.5. The matrix of AA high-calcium FA paste without CCR (Figures 9a-9c) was less dense and loose with a number of non-reacted FA particles embedded. When the mixes contained 20%CCR (Figures 9g-9i), the SEM images showed denser structures than those of the mixes without CCR replacement. Hanjitsuwan et al. [33] and Ismail et al. [48] suggested that CCR comprised mainly of CaO. Therefore, it can react with SiO_2 and Al_2O_3 from high-calcium FA and hence additional C-S-H and C-A-S-H gel coexisted with N-A-S-H gel. Hanjitsuwan et al. [33] also reported that the heat generated from calcium oxide and alkali solutions helped the degree of reaction within the matrix and hence a shorter setting time and a better strength development were obtained as shown in Figures 2 and 3. However, noticeable difference was observed in the mixes of 70FA30CCR-SS/SH=1.0 (Figure 9j), 70FA30CCR-SS/SH=2.0 (Figure 9k) and 70FA30CCR-SS/SH=2.5 (Figure 9l). ~~As mentioned above, less dense pastes were found mainly in the 70FA30CCR-SS/SH=2.5 mix.~~ This seems to be consistent with the XRD patterns shown in Figures 5d, 6d, 7d, 8d). The presences of high amount of Portlandite ($Ca(OH)_2$) and crystalline calcite ($CaCO_3$) would have an adverse effect on the strength development of geopolymer matrix. Hanjitsuwan et al. [33] also found that bottom ash geopolymer mortar incorporated with 30%CCR resulted in carbonate (CO_3^{2-}) band in high wave number in the FTIR spectra analysis. This could explain why they had low compressive and bond strengths.

3.5 Cost analysis and life-cycle assessment

The cost analysis and life-cycle assessment (LCA) of AA high-calcium FA mortar with CCR under different SS-to-SH ratios have been evaluated. Thailand market prices (2018) are used to calculate the price of repair materials. Table 3 shows the prices of AA mortar with and without CCR, while Table 4 shows the prices of PCC and CRM. According to Tables 3 and 4, the total prices of AA high-calcium FA incorporated with CCR, CRM-1, and CRM-2 are about 185-204 £/m^3, 2,208 £/m^3 (1.13 £/kg) and 3,717 £/m^3 (1.76 £/kg), respectively; while the total cost of the base line is about 47 £/m^3. Note that the cost of PCC given in the table is only for the purpose of reference since PCC itself cannot be used as the repair material because it does not have enough bond strength. It can be confirmed with Figure 10 that the use of AA high-calcium FA incorporated with CCR is more cost-effective than the use of CRM. This agreed with previous studies of Phoo-ngernkham et al. [17] and Chindaprasirt et al. [49].

For the LCA analysis, its unit is defined as CO_2-e emitted (t CO_2-e/ton) as reported by the previous study [29]. Based on the literature [37, 50, 51], the emission factors are given in Table 5 and the corresponding results calculated are shown in Tables 6 and 7. It is found that FA gives the lowest value, whereas SS gives the highest value. The mixes with 100FA-SS/SH=1.0, 90FA10CCR-SS/SH=1.0, 80FA20CCR-SS/SH=1.0, and 70FA30CCR-SS/SH=1.0 give the lowest CO_2-e emission, which are 0.237, 0.238, 0.239, and 0.240 ton CO_2-e/ton, respectively. While the CO_2-e emission of the base line, CRM-s, and CRM-2 are 0.722, 11.999, and 11.115 ton CO_2-e/ton, respectively. Based on its low carbon footprint and high cost-effectiveness, the use of AA high-calcium FA incorporated with CCR confirms its suitability as a repair material for concrete in terms of its excellent economic profitability and high bond strength quality.

4. Conclusion

This paper has presented an experimental investigation on the feasibility of using alkali-activated high-calcium FA incorporated with CCR as a potential repair material for repairing damaged concrete. The experimental results include the sitting time, compressive strength, and shear bond strength as well as the effect of % replacement of CCR to FA and SS-to-SH ratio on them. From the results obtained, the following conclusions could be drawn:

1) Both the replacement of FA with CCR and the use of high amount of SS-to-SH ratio can shorten the setting time of AA high-calcium FA mortar. The larger the replacement of FA with CCR or the greater the SS-to-SH ratio used in the mix, the shorter the sitting time is achieved.

2) The compressive strength of the AA high-calcium FA mortar incorporated with CCR increases with increasing CCR replacement. However, this increase vanishes when the replacement of FA with CCR reaches to 20%. After this value the compressive strength of the AA high-calcium FA mortar incorporated with CCR starts to drop. For a fixed replacement of FA with CCR, the compressive strength of the AA high-calcium FA mortar increases with SS-to-SH ratio until SS/SH=2.0. After that value the compressive strength drops with further increased SS/SH ratio, suggesting the maximum value of the SS/SH ratio could be used in the mix is 2.0.

3) The 28-day shear bond strength between the AA mortar and concrete substrate was found to increase with increased CCR replacement or increased SS-to-SH ratio. However, similar to the compressive strength, the increase holds only in the range between 0% and 20% replacement of FA with CCR and the SS/SH ratio being not exceeded 2.0.

4) The XRD results confirmed that the AA high-calcium FA paste samples with an optimum level of CCR replacement and SS-to-SH ratio have increased peaks of $Ca(OH)_2$, C-S-H and broad hump, which correlates to the strength increase. While, the SEM images of

AA pastes with an optimum level of both CCR replacement and SS-to-SH ratio showed an improved microstructure than the pastes without CCR replacement.

5) The cost and life-cycle analyses demonstrated that the AA high-calcium FA mortar with CCR provides a good alternative for repairing damaged concrete, which not only has good performance and low carbon footprint, but also is cost-effective.

Acknowledgements

This work was financially supported by Rajamangala University of Technology Isan, Contact No. NKR2561REV017 and the Thailand Research Fund (TRF) under the TRF Distinguished Research Professor Grant No. DPG6180002. The part of the present work was also supported by the European Commission Research Executive Agency via the Marie Skłodowska-Curie Research and Innovation Staff Exchange Project (689857-PRIGeoC-RISE-2015) and the Industry Academia Partnership Programme-2 (IAPP1617\16) “Development of Sustainable Geopolymer Concrete”. The authors also would like to acknowledge the support of the Department of Civil Engineering, Faculty of Engineering and Architecture, Rajamangala University of Technology Isan, Thailand.

References

[1] Suwan T, Fan M, Braimah N. Micro-mechanisms and compressive strength of Geopolymer-Portland cementitious system under various curing temperatures. Materials Chemistry and Physics. 2016;180:219-25.

[2] Ferreira LFB, Costa HSS, Barata IIA, Santos Júlio ENB, Tiago PMN, Coelho JFJ. Precast alkali-activated concrete towards sustainable construction. Magazine of Concrete Research. 2014;66(12):618-26.

[3] Sadique M, Al-Nageim H, Atherton W, Seton L, Dempster N. Mechano-chemical activation of high-Ca fly ash by cement free blending and gypsum aided grinding. Construction and Building Materials. 2013;43:480-9.

[4] Scrivener K, Martirena F, Bishnoi S, Maity S. Calcined clay limestone cements (LC3). Cement and Concrete Research. 2017.

[5] Bagheri A, Nazari A, Sanjayan JG, Rajeev P. Alkali activated materials vs geopolymers: Role of boron as an eco-friendly replacement. Construction and Building Materials. 2017;146:297-302.

[6] Bakharev T, Sanjayan JG, Cheng YB. Alkali activation of Australian slag cements. Cement and Concrete Research. 1999;29(1):113-20.

[7] Pacheco-Torgal F, Castro-Gomes J, Jalali S. Alkali-activated binders: A review. Part 1. Historical background, terminology, reaction mechanisms and hydration products. Construction and Building Materials. 2008;22(7):1305-14.

[8] Pacheco-Torgal F, Labrincha JA, Leonelli C, Palomo A, Chindaprasirt P. Handbook of Alkali-Activated Cements, Mortars and Concretes ed. 1: WoodHead Publishing Limited- Elsevier Science and Technology; 2014.

[9] Palomo A, Grutzeck MW, Blanco MT. Alkali-activated fly ashes: A cement for the future. Cement and Concrete Research. 1999;29(8):1323-9.

[10] Puertas F, Palacios M, Manzano H, Dolado JS, Rico A, Rodríguez J. A model for the C-A-S-H gel formed in alkali-activated slag cements. Journal of the European Ceramic Society. 2011;31(12):2043-56.

[11] Chindaprasirt P, Paisitsrisawat P, Rattanasak U. Strength and resistance to sulfate and sulfuric acid of ground fluidized bed combustion fly ash–silica fume alkali-activated composite. Advanced Powder Technology. 2014;25(3):1087-93.

[12] Hanjitsuwan S, Phoo-ngernkham T, Li LY, Damrongwiriyanupap N, Chindaprasirt P. Strength development and durability of alkali-activated fly ash mortar with calcium carbide residue as additive. Construction and Building Materials. 2018;162:714-23.

[13] Songpiriyakij S, Pulngern T, Pungpremtrakul P, Jaturapitakkul C. Anchorage of steel bars in concrete by geopolymer paste. Materials & Design. 2011;32(5):3021-8.

[14] Sarker PK. Bond strength of reinforcing steel embedded in fly ash-based geopolymer concrete. Materials and Structures/Materiaux et Constructions. 2011;44(5):1021-30.

[15] Sarker PK, Kelly S, Yao Z. Effect of fire exposure on cracking, spalling and residual strength of fly ash geopolymer concrete. Materials & Design. 2014;63(0):584-92.

[16] Phoo-ngernkham T, Hanjitsuwan S, Damrongwiriyanupap N, Chindaprasirt P. Effect of sodium hydroxide and sodium silicate solutions on strengths of alkali activated high calcium fly ash containing Portland cement. KSCE Journal of Civil Engineering. 2017;21(6):2202-10.

[17] Phoo-ngernkham T, Hanjitsuwan S, Li LY, Damrongwiriyanupap N, Chindaprasirt P. Adhesion characterization of Portland cement concrete and alkali-activated binders under different types of calcium promoters. Advances in Cement Research. 2019;31(2):69-79.

[18] Phoo-ngernkham T, Sata V, Hanjitsuwan S, Ridtirud C, Hatanaka S, Chindaprasirt P. High calcium fly ash geopolymer mortar containing Portland cement for use as repair material. Construction and Building Materials. 2015;98:482-8.

[19] Davidovits J. Geopolymers - Inorganic polymeric new materials. Journal of Thermal Analysis. 1991;37(8):1633-56.

[20] Garcia-Lodeiro I, Fernandez-Jimenez A, Palomo A. Hydration kinetics in hybrid binders: Early reaction stages. Cement and Concrete Composites. 2013;39(0):82-92.

[21] Kumar S, Kumar R, Mehrotra SP. Influence of granulated blast furnace slag on the reaction, structure and properties of fly ash based geopolymer. Journal of Materials Science. 2010;45(3):607-15.

[22] Puertas F, Martínez-Ramírez S, Alonso S, Vázquez T. Alkali-activated fly ash/slag cements: Strength behaviour and hydration products. Cement and Concrete Research. 2000;30(10):1625-32.

[23] Rashad AM. Properties of alkali-activated fly ash concrete blended with slag. Iranian Journal of Materials Science and Engineering. 2013;10(1):57-64.

[24] Phoo-ngernkham T, Maegawa A, Mishima N, Hatanaka S, Chindaprasirt P. Effects of sodium hydroxide and sodium silicate solutions on compressive and shear bond strengths of FA–GBFS geopolymer. Construction and Building Materials. 2015;91(0):1-8.

[25] Phoo-ngernkham T, Chindaprasirt P, Sata V, Hanjitsuwan S, Hatanaka S. The effect of adding nano-SiO_2 and nano-Al_2O_3 on properties of high calcium fly ash geopolymer cured at ambient temperature. Materials & Design. 2014;55(0):58-65.

[26] Phoo-ngernkham T, Chindaprasirt P, Sata V, Pangdaeng S, Sinsiri T. Properteis of high calcium fly ash geopolymer pastes containing Portland cement as additive. International Journal of Minerals, metallurgy and Materials. 2013;20(2):214-20.

[27] Phoo-ngernkham T, Chindaprasirt P, Sata V, Sinsiri T. High calcium fly ash geopolymer containing diatomite as additive. Indian Journal of Engineering & Materials Sciences. 2013;20(4):310-8.

[28] Phoo-ngernkham T, Sata V, Hanjitsuwan S, Ridtirud C, Hatanaka S, Chindaprasirt P. Compressive strength, Bending and Fracture Characteristics of High Calcium Fly

Ash Geopolymer Mortar Containing Portland Cement Cured at Ambient Temperature. Arabian Journal for Science and Engineering. 2016;41(4):1263-71.

[29] Phoo-ngernkham T, Hanjitsuwan S, Suksiripattanapong C, Thumrongvut J, Suebsuk J, Sookasem S. Flexural strength of notched concrete beam filled with alkali-activated binders under different types of alkali solutions. Construction and Building Materials. 2016;127:673-8.

[30] Pangdaeng S, Phoo-ngernkham T, Sata V, Chindaprasirt P. Influence of curing conditions on properties of high calcium fly ash geopolymer containing Portland cement as additive. Materials & Design. 2014;53(0):269-74.

[31] Boonserm K, Sata V, Pimraksa K, Chindaprasirt P. Microstructure and strength of blended FBC-PCC fly ash geopolymer containing gypsum as an additive. ScienceAsia. 2012;38(2):175-81.

[32] Boonserm K, Sata V, Pimraksa K, Chindaprasirt P. Improved geopolymerization of bottom ash by incorporating fly ash and using waste gypsum as additive. Cement and Concrete Composites. 2012;34(7):819-24.

[33] Hanjitsuwan S, Phoo-ngernkham T, Damrongwiriyanupap N. Comparative Study using Portland Cement and Calcium Carbide Residue as a Promoter in Bottom Ash Geopolymer Mortar. Construction and Building Materials. 2017;133:128-34.

[34] Makaratat N, Jaturapitakkul C, Namarak C, Sata V. Effects of binder and $CaCl_2$ contents on the strength of calcium carbide residue-fly ash concrete. Cement and Concrete Composites. 2011;33(3):436-43.

[35] Amnadnua K, Tangchirapat W, Jaturapitakkul C. Strength, water permeability, and heat evolution of high strength concrete made from the mixture of calcium carbide residue and fly ash. Materials & Design. 2013;51:894-901.

[36] Phummiphan I, Horpibulsuk S, Phoo-ngernkham T, Arulrajah A, Shen SL. Marginal Lateritic Soil Stabilized with Calcium Carbide Residue and Fly Ash Geopolymers as a Sustainable Pavement Base Material. Journal of Materials in Civil Engineering. 2016;0(0):04016195.

[37] Phetchuay C, Horpibulsuk S, Arulrajah A, Suksiripattanapong C, Udomchai A. Strength development in soft marine clay stabilized by fly ash and calcium carbide residue based geopolymer. Applied Clay Science. 2016;127–128:134-42.

[38] ASTM C618-15. Standard specification for coal fly ash and raw or calcined natural pozzolan for use in concrete. Annual Book of ASTM Standard. 2015;Vol.04.02.

[39] ASTM C191-13. Standard test method for time of setting of hydrualic cement by vicat needle. Annual Book of ASTM Standard 2013;Vol.04.01.

[40] ASTM C109. Standard test method of compressive strength of hydrualic cement mortars (using 2-in. or [50 mm] cube speciments). Annual Book of ASTM Standard. 2002;Vol.04.01.

[41] ASTM C882. Standard test method for bond strength of epoxy-resin systems used with concrete by slant shear. Annual Book of ASTM Standard. 2005;Vol.04.02.

[42] Phoo-ngernkham T, Hanjitsuwan S, Thumrongvut J, Detphan S, Suksiripattanapong S, Damrongwiriyanupap N, et al. Shear bond strength of FA-PC geopoylmer under different sand to binder ratios and sodium hydroxide concentrations. International Journal of GEOMATE. 2018;14(52):52-7.

[43] Lee WKW, Van Deventer JSJ. The effects of inorganic salt contamination on the strength and durability of geopolymers. Colloids and Surfaces A: Physicochemical and Engineering Aspects. 2002;211(2-3):115-26.

[44] ASTM C881/C881M-14. Standard specification for epoxy-resin-base bonding systems for concrete. Annual Book of ASTM Standard. 2014;Vol.04.02.

[45] Khater H. Effect of calcium on geopolymerization of aluminosilicate wastes. Journal of Materials in Civil Engineering. 2012;24(1):92-101.

[46] ASTM C928-13. Standard specification for packaged, dry, rapid-hardening cementitious materials for concrete repairs. Annual Book of ASTM Standard. 2013;Vol.04.02.

[47] Pacheco-Torgal F, Castro-Gomes JP, Jalali S. Adhesion characterization of tungsten mine waste geopolymeric binder. Influence of OPC concrete substrate surface treatment. Construction and Building Materials. 2008;22(3):154-61.

[48] Ismail I, Bernal SA, Provis JL, San Nicolas R, Hamdan S, van Deventer JSJ. Modification of phase evolution in alkali-activated blast furnace slag by the incorporation of fly ash. Cement and Concrete Composites. 2014;45(0):125-35.

[49] Chindaprasirt P, Phoo-ngernkham T, Hanjitsuwan S, Horpibulsuk S, Poowancum A, Injorhor B. Effect of calcium-rich compounds on setting time and strength development of alkali-activated fly ash cured at ambient temperature. Case Studies in Construction Materials. 2018:e00198.

[50] Turner LK, Collins FG. Carbon dioxide equivalent (CO_2-e) emissions: A comparison between geopolymer and OPC cement concrete. Construction and Building Materials. 2013;43(0):125-30.

[51] Collins FG. Inclusion of carbonation during the life cycle of built and recycled concrete: influence on their carbon footprint. The International Journal of Life Cycle Assessment. 2010;15(6):549-56.

Table 1 Chemical compositions of FA and CCR (by weight)

Materials	SiO_2	Al_2O_3	Fe_2O_3	CaO	MgO	K_2O	Na_2O	Other	SO_3	LOI
FA	31.32	13.96	15.64	25.79	2.94	2.93	2.83	-	3.29	1.30
CCR	6.16	3.54	0.18	89.24	0.37	-	-	0.50	0.87	2.79

Table 2 Mix proportions of alkali-activated high calcium FA mortar with CCR (kg/m^3)

Mix No.	Mix symbol	FA (kg)	CCR (kg)	Sand (kg)	SH (kg)	SS (kg)
1	100FA-SS/SH=1.0	830	-	817	255	255
2	100FA-SS/SH=1.5	832	-	820	205	307
3	100FA-SS/SH=2.0	834	-	821	171	342
4	100FA-SS/SH=2.5	835	-	822	147	367
5	90FA10CCR-SS/SH=1.0	743	83	814	254	254
6	90FA10CCR-SS/SH=1.5	745	83	816	204	306
7	90FA10CCR-SS/SH=2.0	747	83	818	170	340
8	90FA10CCR-SS/SH=2.5	747	83	818	146	365
9	80FA20CCR-SS/SH=1.0	657	164	809	253	253
10	80FA20CCR-SS/SH=1.5	660	164	812	203	304
11	80FA20CCR-SS/SH=2.0	660	164	813	169	338
12	80FA20CCR-SS/SH=2.5	661	164	814	145	363
13	70FA30CCR-SS/SH=1.0	572	245	805	251	251
14	70FA30CCR-SS/SH=1.5	574	245	808	202	303
15	70FA30CCR-SS/SH=2.0	575	245	809	168	336
16	70FA30CCR-SS/SH=2.5	575	245	810	145	361

Table 3 Prices of alkali-activated high-calcium FA with CCR

Mix symbol	FA (£)	CCR (£)	Sand (£)	SH (£)	SS (£)	Total price (£/m^3)
100FA-SS/SH=1.0	39.5	0	7.0	60.7	85.0	192
100FA-SS/SH=1.5	39.6	0	7.0	48.8	102.3	198
100FA-SS/SH=2.0	39.7	0	7.0	40.7	114.0	202
100FA-SS/SH=2.5	39.8	0	7.0	35.0	122.3	204
90FA10CCR-SS/SH=1.0	35.4	1.0	7.0	60.5	84.7	188
90FA10CCR-SS/SH=1.5	35.5	1.0	7.0	48.6	102.0	194
90FA10CCR-SS/SH=2.0	35.6	1.0	7.0	40.5	113.3	197
90FA10CCR-SS/SH=2.5	35.6	1.0	7.0	34.8	121.7	200
80FA20CCR-SS/SH=1.0	31.3	2.0	6.9	60.2	84.3	185
80FA20CCR-SS/SH=1.5	31.4	2.0	7.0	48.3	101.3	190
80FA20CCR-SS/SH=2.0	31.4	2.0	7.0	40.2	112.7	193
80FA20CCR-SS/SH=2.5	31.5	2.0	7.0	34.5	121.0	196
70FA30CCR-SS/SH=1.0	27.2	2.9	6.9	59.8	83.7	180
70FA30CCR-SS/SH=1.5	27.3	2.9	6.9	48.1	101.0	186
70FA30CCR-SS/SH=2.0	27.4	2.9	6.9	40.0	112.0	189
70FA30CCR-SS/SH=2.5	27.4	2.9	6.9	34.5	120.3	192

Table 4 Prices of PCC and CRM

Mix symbol	PC (£)	Fine aggregate (£)	Coarse aggregate (£)	CRM (£)	Water (£)	Total price (£/m^3)
PCC (base line)	28.7	4.5	8.0	-	5.8	47
CRM-1	-	-	-	3,709.0	8.0	3,717
CRM-2	-	-	-	2,195.5	12.5	2,208

Table 5 The emission factors of tested materials [37, 50, 51].

Materials	Emission factor (t CO_2-e/ton)
Portland cement, PC (kg)	0.8200
River sand, RS (kg)	0.0139
Coarse aggregate, CA (kg)	0.4300
Commercial repair material, CRM (kg)	5.7000
Fly ash, FA (kg)	0.0070
Calcium carbide residue, CCR (kg)	0.0350
Sodium hydroxide, SH (kg)	0.7000
Sodium silicate, SS (kg)	1.5140

Table 6 LCA analysis of alkali-activated high-calcium FA with CCR from this study

Mix symbol	FA (kg)	CO_2-e/t from FA	CCR (kg)	CO_2-e/t from CCR	RS (kg)	CO_2-e/t from RS	SH (kg)	CO_2-e/t from SH	SS (kg)	CO_2-e/t from SS	Total CO_2-e/t
100FA-SS/SH=1.0	830	0.0058	-	-	817	0.0114	255	0.0536	255	0.1660	0.237
100FA-SS/SH=1.5	832	0.0058	-	-	820	0.0114	205	0.0431	307	0.1999	0.260
100FA-SS/SH=2.0	834	0.0058	-	-	821	0.0114	171	0.0359	342	0.2226	0.276
100FA-SS/SH=2.5	835	0.0058	-	-	822	0.0114	147	0.0309	367	0.2389	0.287
90FA10CCR-SS/SH=1.0	743	0.0052	83	0.0029	814	0.0113	254	0.0533	254	0.1654	0.238
90FA10CCR-SS/SH=1.5	745	0.0052	83	0.0029	816	0.0113	204	0.0428	306	0.1992	0.262
90FA10CCR-SS/SH=2.0	747	0.0052	83	0.0029	818	0.0114	170	0.0357	340	0.2213	0.277
90FA10CCR-SS/SH=2.5	747	0.0052	83	0.0029	818	0.0114	146	0.0307	365	0.2376	0.288
80FA20CCR-SS/SH=1.0	657	0.0046	164	0.0057	809	0.0112	253	0.0531	253	0.1647	0.239
80FA20CCR-SS/SH=1.5	660	0.0046	164	0.0058	812	0.0113	203	0.0426	304	0.1979	0.262
80FA20CCR-SS/SH=2.0	660	0.0046	164	0.0058	813	0.0113	169	0.0355	338	0.2200	0.277
80FA20CCR-SS/SH=2.5	661	0.0046	164	0.0058	814	0.0113	145	0.0305	363	0.2363	0.288
70FA30CCR-SS/SH=1.0	572	0.0040	245	0.0086	805	0.0112	251	0.0527	251	0.1634	0.240
70FA30CCR-SS/SH=1.5	574	0.0040	245	0.0086	808	0.0112	202	0.0426	303	0.1973	0.264
70FA30CCR-SS/SH=2.0	575	0.0040	245	0.0086	809	0.0112	168	0.0353	336	0.2187	0.278
70FA30CCR-SS/SH=2.5	575	0.0040	245	0.0086	810	0.0113	145	0.0305	361	0.2350	0.289

Table 7 LCA analysis of PCC and CRM from this study

Mix symbol	PC (kg)	CO_2-e/t from PC	RS (kg)	CO_2-e/t from RS	CA (kg)	CO_2-e/t from CA	CRM (kg)	CO_2-e/t from CRM	Total CO_2-e/t
Base line	495	0.1040	510	0.0071	938	0.6107	-	-	0.722
CRM-1	-	-	-	-	-	-	2105	11.999	11.999

CRM-2	-	-	-	-	-	-	1950	11.115	11.115

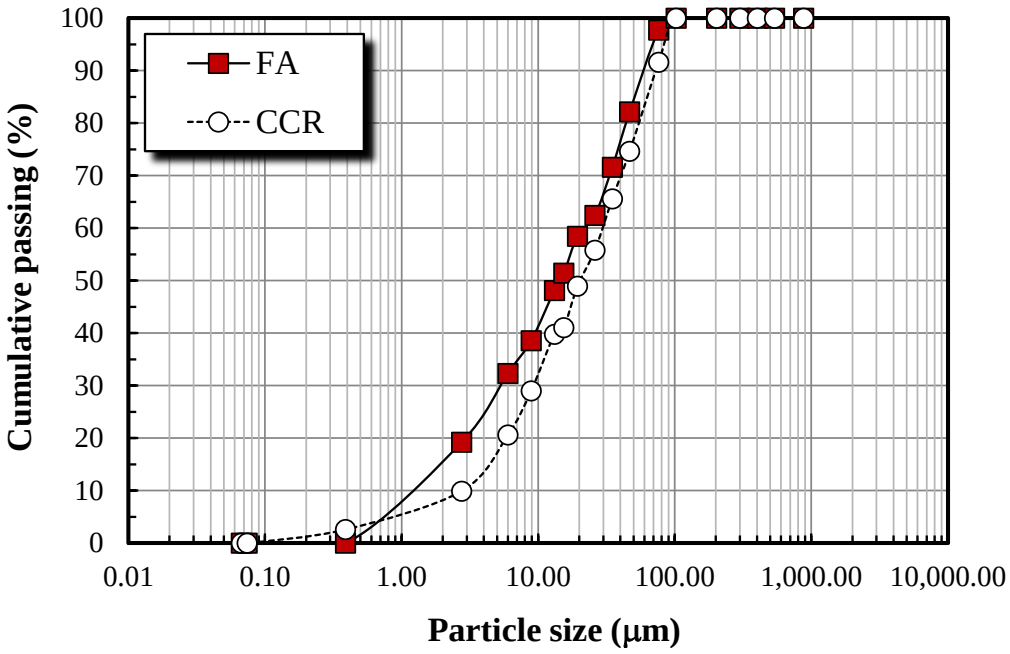

Figure 1 Particle size distributions of FA and CCR.

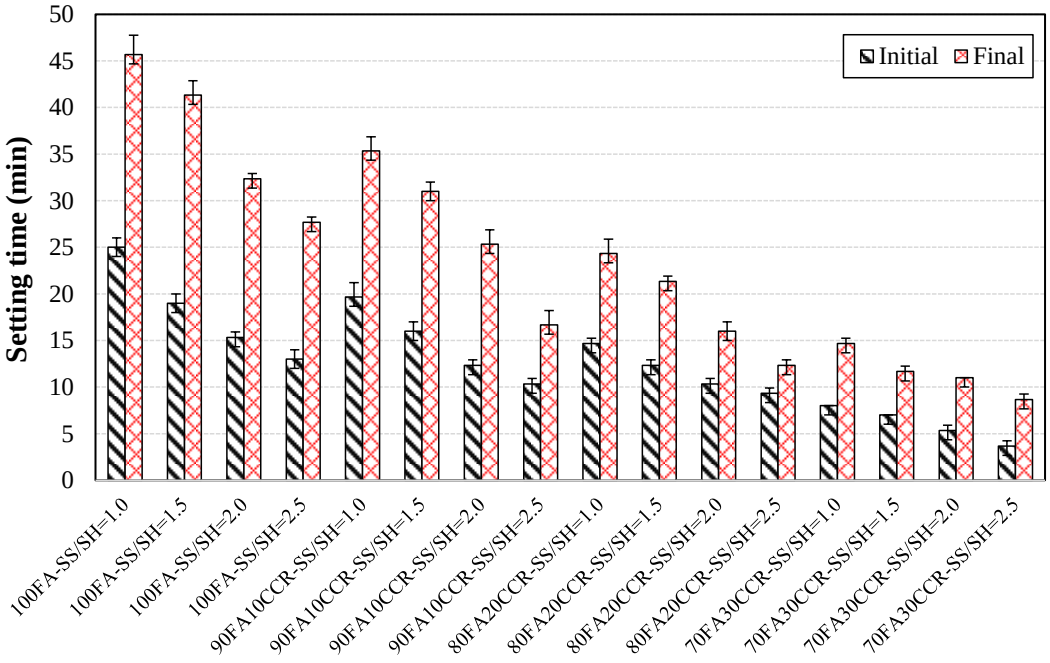

Figure 2 Setting time of alkali-activated high-calcium FA mortar under different CCR replacement levels and SS-to-SH ratios

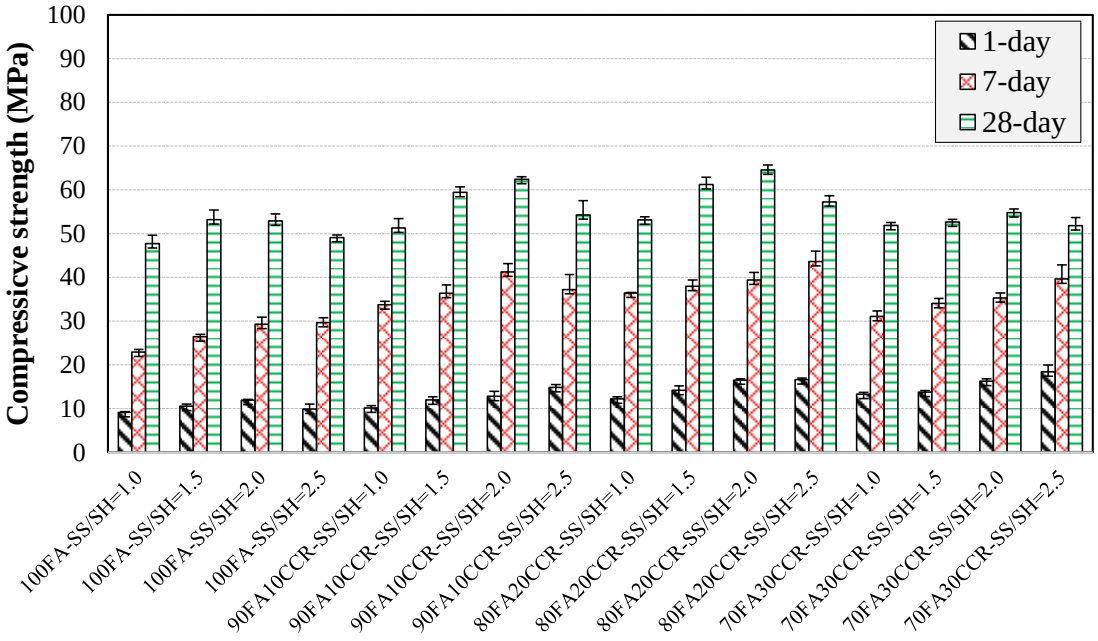

Figure 3 Compressive strength of alkali-activated high-calcium FA mortar incorporated with CCR under different SS-to-SH ratios and curing times

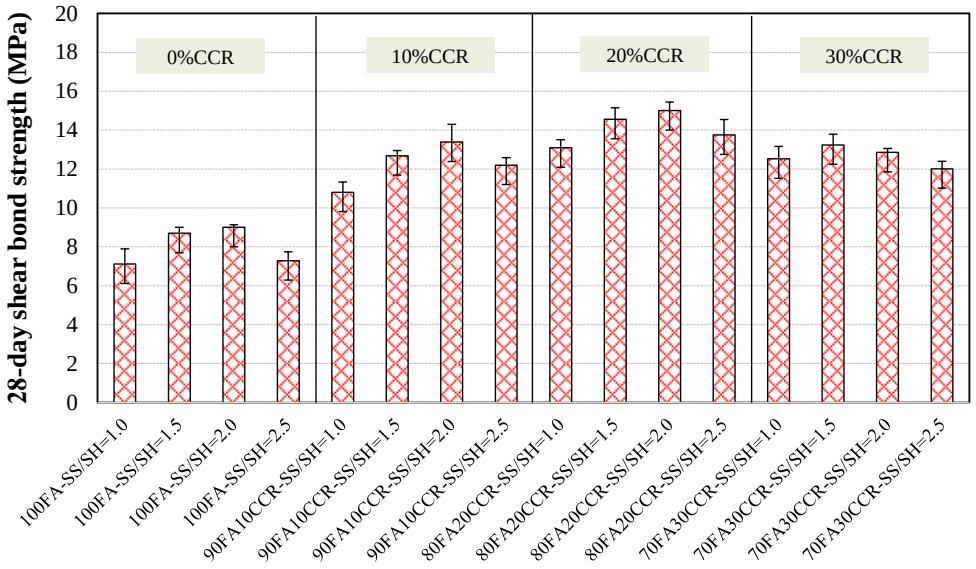

Figure 4 28-day shear bond strength between PCC substrate and alkali-activated high-calcium FA mortar under different CCR replacement levels and SS-to-SH ratios

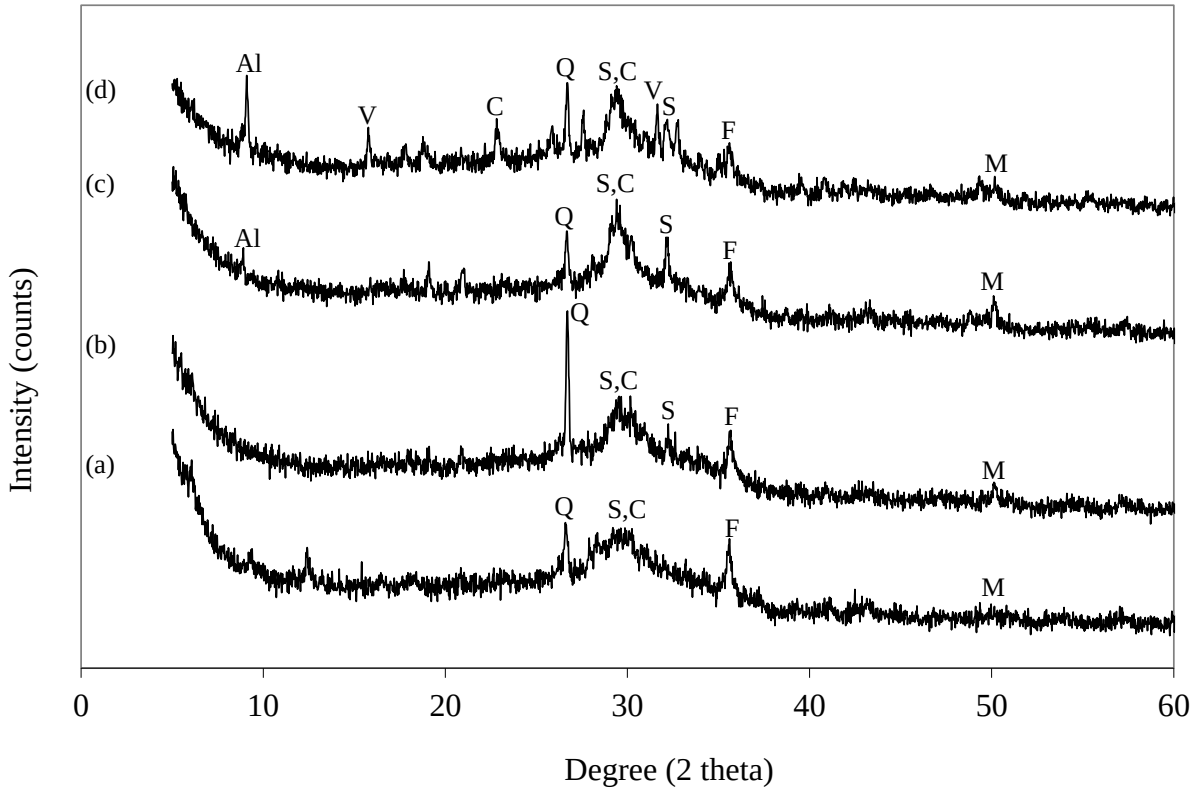

Q=Quartz (SiO_2), F=Magnetite (Fe_3O_4), S=Calcium silicate hydrate (C-S-H), Al=aluminite ($Al_2(SO_4)(OH)_4.17H_2O$), V=Vishnevite ($Na_8Al_6Si_6O_{24}(SO_4)_2.H_2O$), C=Calcite ($CaCO_3$), P = Portlandite ($Ca(OH)_2$), M = Mullite ($Al_6Si_2O_{13}$)

Figure 5 XRD patterns of alkali-activated high-calcium FA paste incorporated with CCR at SS-to-SH ratio of 1.0, cured for 28 days: curve labelled (a) 100FA-SS/SH=1.0; (b) 90FA10CCR-SS/SH=1.0; (c) 80FA20CCR-SS/SH=1.0; (d) 70FA30CCR-SS/SH=1.0

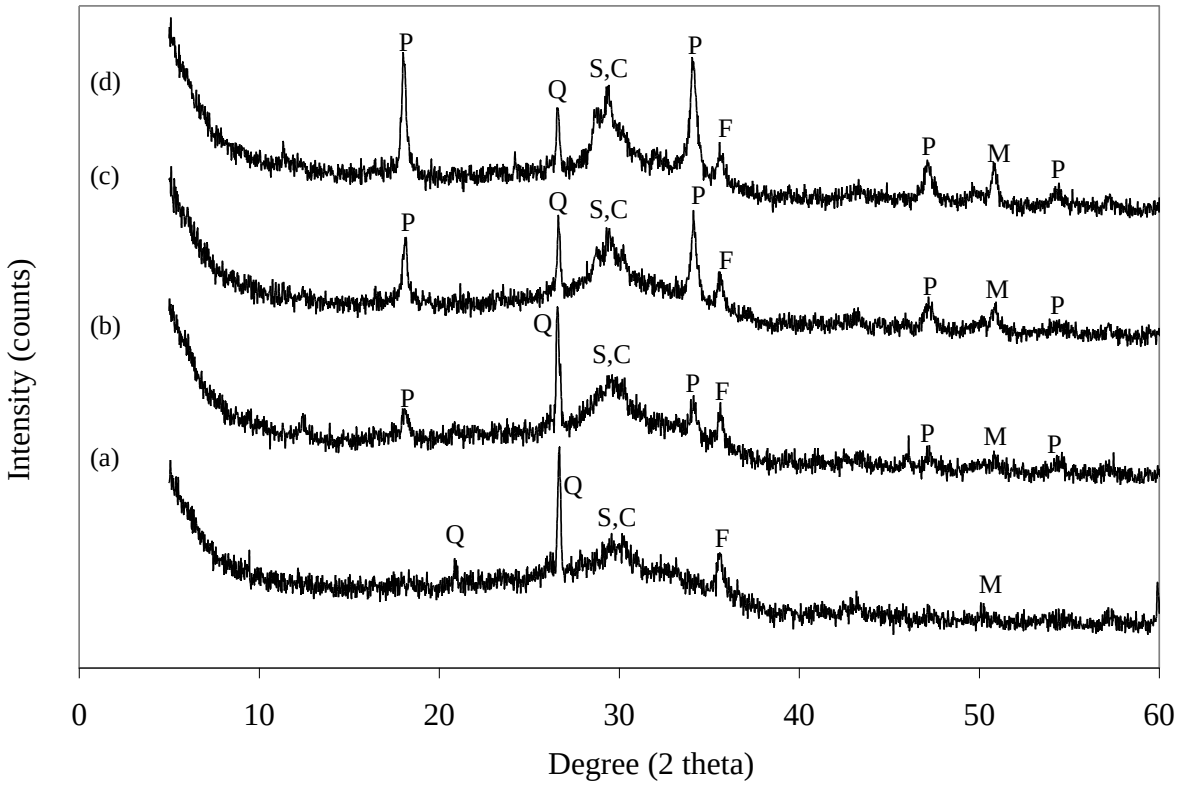

Q=Quartz (SiO_2), F=Magnetite (Fe_3O_4), S=Calcium silicate hydrate ($Ca_{15}SiO_{3.5}\,xH_2O$), C=Calcite ($CaCO_3$),
P = Portlandite ($Ca(OH)_2$), M = Mullite ($Al_6Si_2O_{13}$)

Figure 6 XRD patterns of alkali-activated high-calcium FA paste incorporated with CCR at SS-to-SH ratio of 1.5, cured for 28 days: curve labelled (a) 100FA-SS/SH=1.5; (b) 90FA10CCR-SS/SH=1.5; (c) 80FA20CCR-SS/SH=1.5; (d) 70FA30CCR-SS/SH=1.5

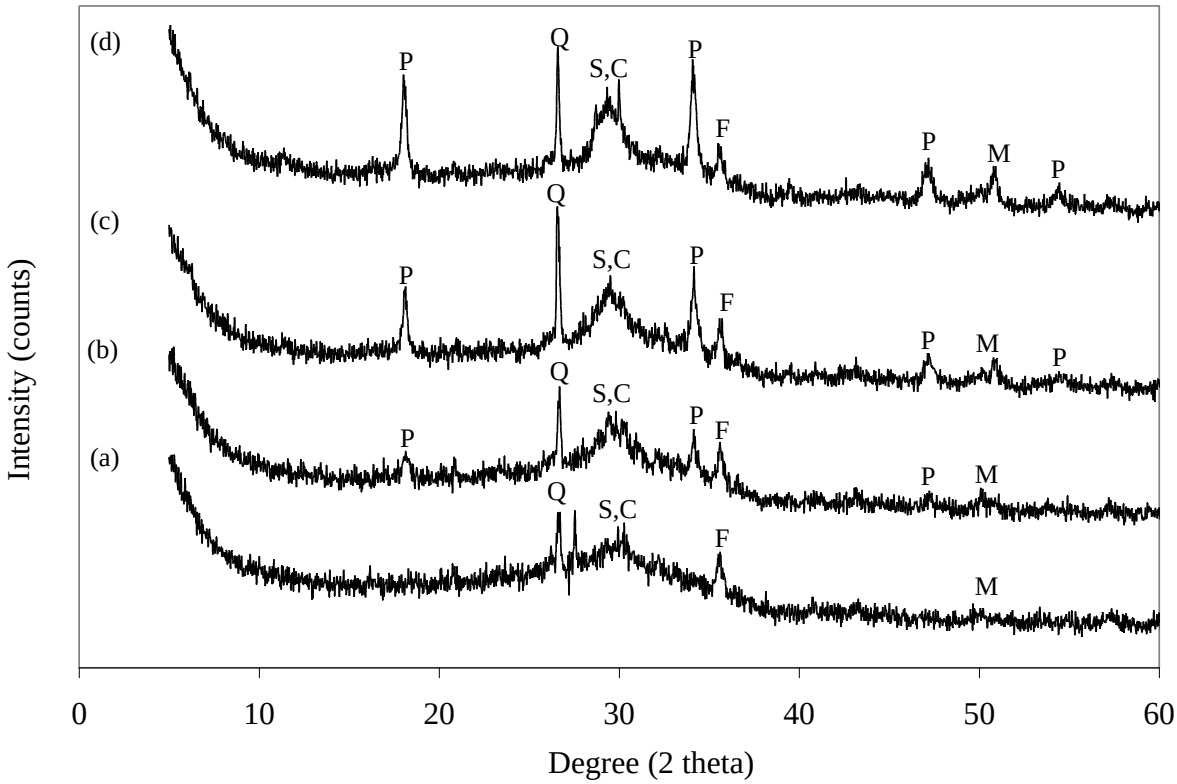

Q=Quartz (SiO_2), F=Magnetite (Fe_3O_4), S=Calcium silicate hydrate ($Ca_{15}SiO_{3.5}\,xH_2O$), C=Calcite ($CaCO_3$),
P = Portlandite ($Ca(OH)_2$), M = Mullite ($Al_6Si_2O_{13}$)

Figure 7 XRD patterns of alkali-activated high-calcium FA paste incorporated with CCR at SS-to-SH ratio of 2.0, cured for 28 days: curve labelled (a) 100FA-SS/SH=2.0; (b) 90FA10CCR-SS/SH=2.0; (c) 80FA20CCR-SS/SH=2.0; (d) 70FA30CCR-SS/SH=2.0

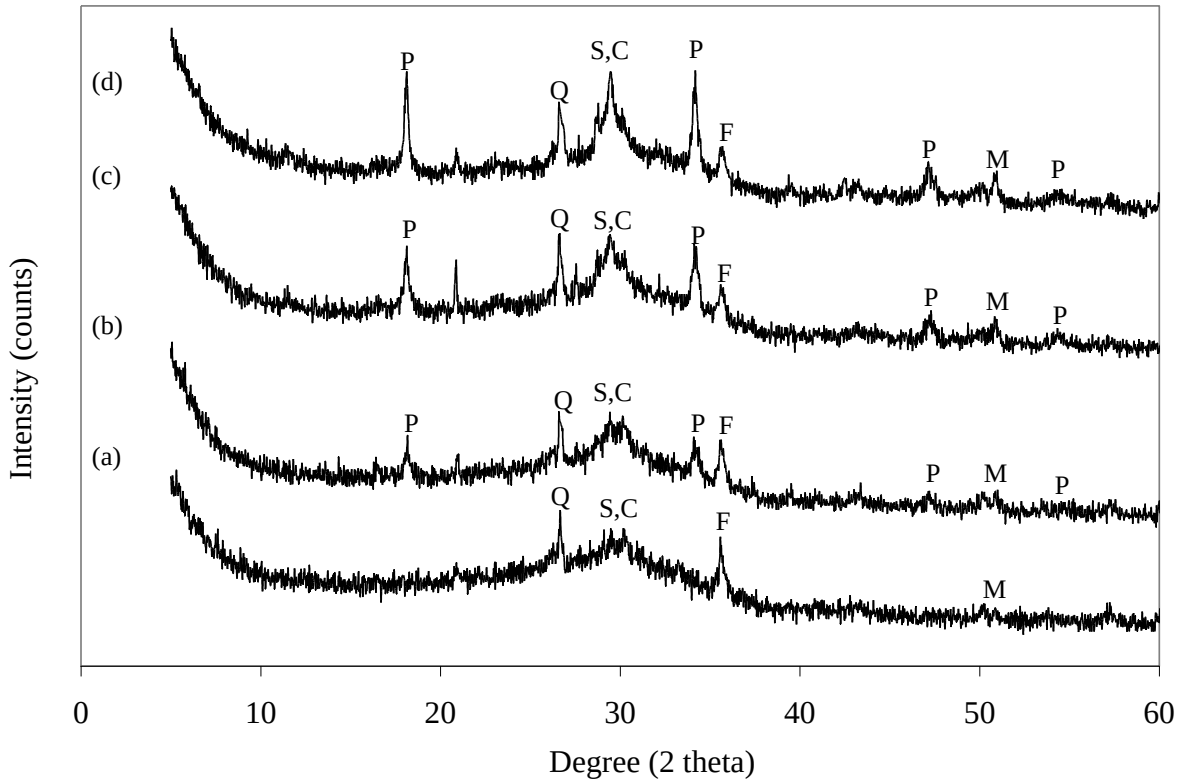

Q=Quartz (SiO_2), F=Magnetite (Fe_3O_4), S=Calcium silicate hydrate ($Ca_{15}SiO_{3.5}\,xH_2O$), C=Calcite ($CaCO_3$),
P = Portlandite ($Ca(OH)_2$), M = Mullite ($Al_6Si_2O_{13}$)

Figure 8 XRD patterns of alkali-activated high-calcium FA paste incorporated with CCR at SS-to-SH ratio of 2.5, cured for 28 days: curve labelled (a) 100FA-SS/SH=2.5; (b) 90FA10CCR-SS/SH=2.5; (c) 80FA20CCR-SS/SH=2.5; (d) 70FA30CCR-SS/SH=2.5

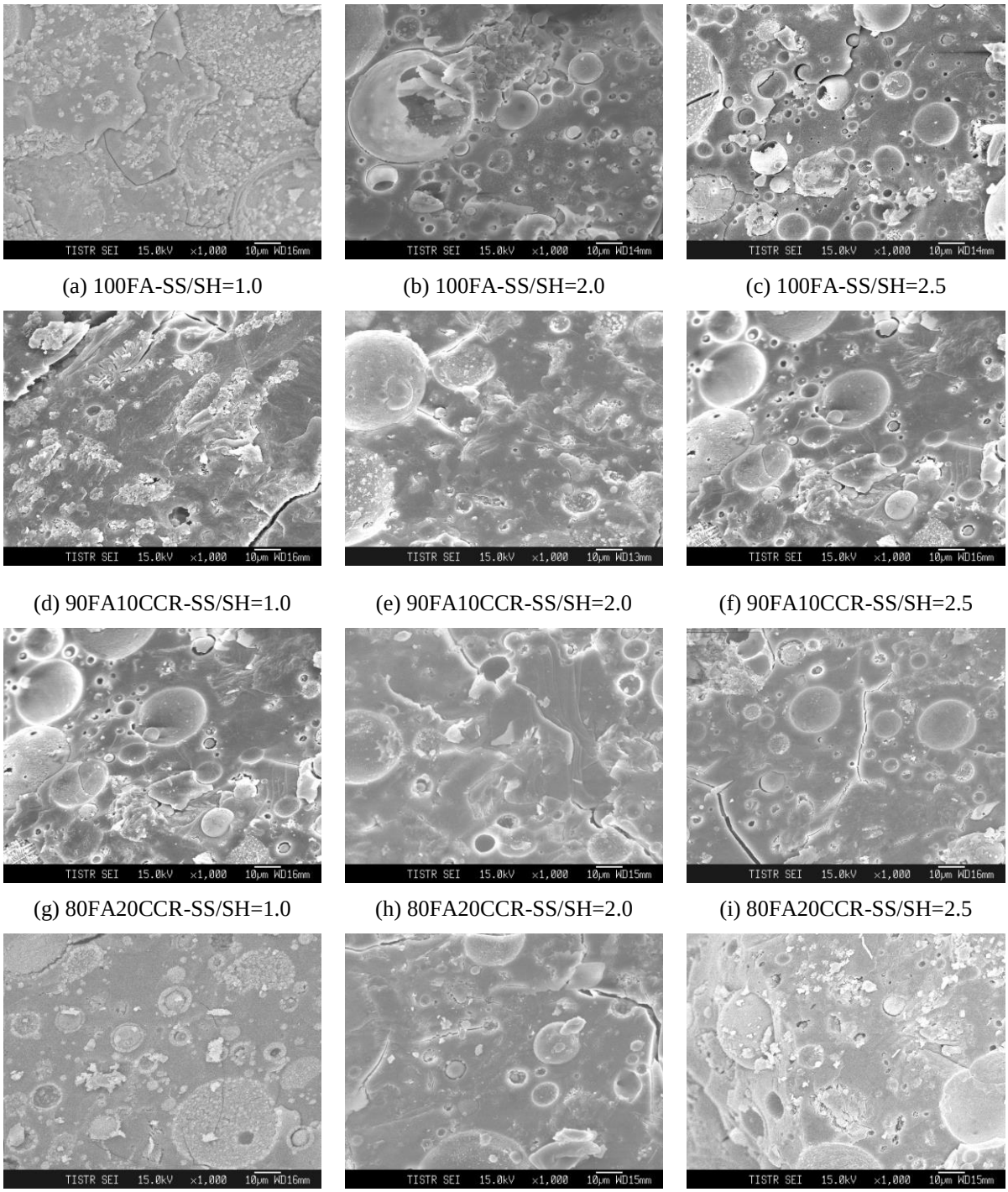

(a) 100FA-SS/SH=1.0 (b) 100FA-SS/SH=2.0 (c) 100FA-SS/SH=2.5

(d) 90FA10CCR-SS/SH=1.0 (e) 90FA10CCR-SS/SH=2.0 (f) 90FA10CCR-SS/SH=2.5

(g) 80FA20CCR-SS/SH=1.0 (h) 80FA20CCR-SS/SH=2.0 (i) 80FA20CCR-SS/SH=2.5

(j) 70FA30CCR-SS/SH=1.0 (k) 70FA30CCR-SS/SH=2.0 (l) 70FA30CCR-SS/SH=2.5

Figure 9 SEM images of alkali-activated high-calcium FA paste under different CCR replacement levels and SS-to-SH ratios, cured for 28 days

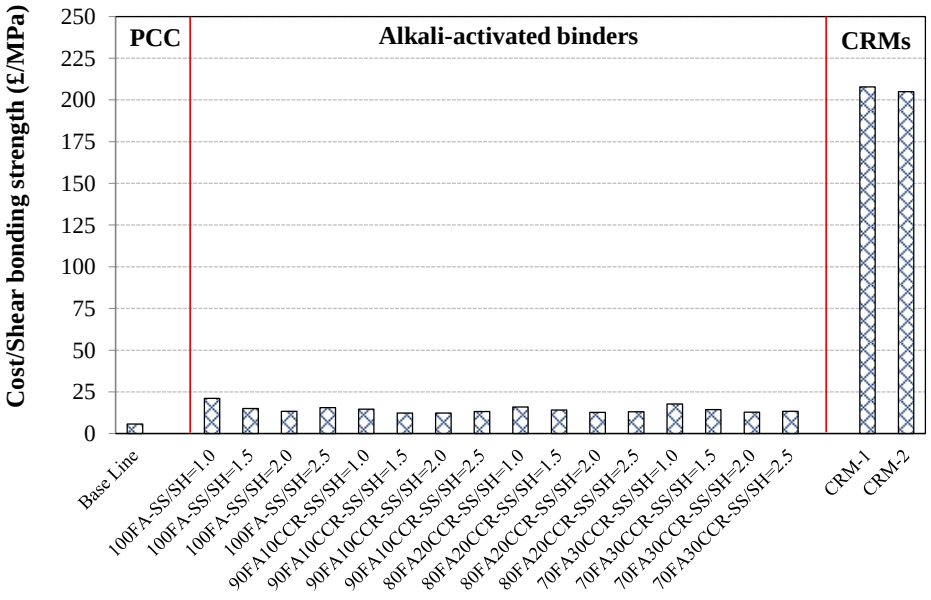

Figure 10 Comparison of cost-effective between alkali-activated high-calcium FA with CCR mortar under different SS-to-SH ratios and commercial repair material.